JMEPEG (2010) 19:627–632
DOI: 10.1007/s11665-009-9517-4

1059-9495/$19.00

Effect of Laser Texturing on the Microstructure and Textures of 1050 Aluminum Alloy

Chunbo Cai, Zesheng Ji, and Huajun Zhang

(Submitted March 13, 2009; in revised form June 13, 2009)

To improve the surface morphology, formability, and deep drawing properties of 1050 aluminum alloy sheets, laser-textured rolls were used in cold rolling process. Effects of laser-textured rolls, comparing with conventional ones, on microstructure and texture of aluminum alloys after rolling and following recrystallization were studied. In aluminum sheets processed by laser-textured rolls and conventional rolls, microstructure and texture were similar after rolling, but significantly different after recrystallization. Laser texturing process results in finer and inhomogeneous recrystallized grains. The recrystallization texture of the specimen rolled with conventional roll has a major cube component and a minor R component. The intensity of cube component increases with increasing annealing temperature. However, recrystallization texture of the specimen rolled with laser-textured roller is much more random. The specimen shows that recrystallization texture has only a weak cube orientation but strong rotated-cube orientation as well as a much higher fraction of random orientation.

Keywords 1050 aluminum alloy, laser texturing, recrystallization, texture

1. Introduction

Laser texturing technique has been widely used in rolling of steel and aluminum sheets to improve surface morphology, formability, and deep drawing properties of bands (Ref 1, 2). During rolling with laser-textured roll (LTR), morphology of roll is copied to sheet surface. The imposed deformation causes friction in the deformation zone and results in inhomogeneous deformation on the surface of the sheet. Comparing to conventional roll (CR) processing, the friction between roll and sheet in LTR processing is high. Therefore, microstructure and deformation textures of LTR-rolled sheets are different from those of CR-rolled sheets. Recent studies have shown that the LTR technology can control the surface morphology and improve formability (Ref 3, 4). But the effects of LTR on texture of aluminum alloy have not been investigated.

The texture of aluminum alloys processed to sheet by CR rolling processes is generally dominated by components called β-fiber. This is represented by a continuous tube of orientations that runs from the {110}⟨112⟩ (brass orientation) through the {123}⟨634⟩ (S orientation) to the {112}⟨111⟩ (copper orientation). Most of previous investigations (Ref 5-10) have shown that the β-fiber texture transforms to cube-dominated texture after annealing treatment. In LTR rolling processes, the crater morphology on the textured roll surface can cut through the rolling strip, which results in inhomogeneous deformation on the sheet surface. The inhomogeneous deformation will affect the orientation of the recrystallized grains during annealing. Annealing temperature will also influence recrystallization texture. In this research, effects of laser texturing on microstructure and texture during annealing are investigated in 1050 aluminum alloy.

Chunbo Cai, Zesheng Ji, and **Huajun Zhang**, Department of Materials Science and Engineering, Harbin University of Science and Technology, Harbin 150040, China. Contact e-mail: caichunbo@126.com.

2. Experimental

The material used in this investigation is a commercially produced hot bands of 1050 aluminum alloy. Chemical composition of the alloy is shown in Table 1. The slab is hot rolled to 7.0 mm at 480 °C. The hot band is subsequently cold rolled on a laboratory rolling mill with CR (Ra: 0.227 μm) and LTR (Ra: 1.024 μm) to 0.5 mm final thickness in seven passes. Final thickness reduction of 93 pct is used. Finally, the cold-rolled specimens are annealed at temperatures ranging from 240 to 400 °C for 1 h. Then, the samples are cut into 20 mm × 20 mm to be ready for microstructural observation and texture testing.

Microstructural examinations are carried out using an Olympus (Melville, NY) inverted metallurgical microscopy. The samples are cut from longitudinal sections as defined by rolling direction (RD) and normal direction (ND). After mechanical grinding and polishing, the samples are electropolished at a voltage of 28 V DC for 5 s using 10 mL $HClO_4$ and 90 mL CH_3OH followed by anodizing at a voltage of 20 V DC for 15 s using 38 mL H_2SO_4-43 mL H_3PO_4-19 mL H_2O.

Crystallographic textures of rolled and recrystallized sheets are measured at the surface of sheets by the Schulz reflection method on a PW3040/60-type X-ray goniometer, using CuK_α radiation. The goniometer was operated at 40 kV and 20 mA. Three incomplete pole figures {111}, {200}, and {220} ($0° \le \alpha \le 75°$) are measured. The orientation distribution functions (ODFs) are calculated from the incomplete pole

Table 1 Composition of 1050 aluminum alloy (mass fraction, %)

Si	Fe	Cu	Ti	Mg	Al
0.071	0.250-0.350	0.001	0.020-0.030	<0.001	Bal.

figures using the series expansion method (l_{max} = 16) (Ref 11). The ODFs are presented as plots of constant ϕ_2 sections with isointensity contours in Euler space defined by the Euler angles ϕ_1, Φ, and ϕ_2.

3. Results

3.1 Microstructures and Texture of the Hot Band and Cold-Rolled Samples

Figure 1 shows the cross section microstructure of different samples. The microstructure of hot band shows a typical pancake grain structure. Some fine recrystallized grains are observed in the hot band. After a 93 pct reduction, a typical deformed structure is developed, and the grains of CR- and LTR-deformed samples are significantly deformed in the RD. The grain structures of the samples are similar.

Figure 2 shows the ODFs of the hot band and 93 pct reduction rolled by CR and LTR. The alloy contains strong {001}⟨110⟩ shear component. In two cold-rolled specimens, the well-known copper-type rolling texture is formed, which is characterized by the development of preferred orientations along β-fiber running from the Cu-orientation {112}⟨111⟩ over the S-orientation {123}⟨634⟩ to the Bs-orientation {011}⟨211⟩ (Ref 12). It must be emphasized that the intensity distributions of this rolling textures are very similar for both samples. Only in the low-intensity regions some difference are obtained. Furthermore, no noticeable through-thickness variation of the cold rolling textures in both specimens is found.

3.2 Recrystallization of Cold-Rolled Samples

3.2.1 The Change of Recrystallized Structure. A typical microstructure evolution of CR- and LTR-rolled samples with annealing at 280, 320, and 360 °C for 1 h is shown in Fig. 3 and 4. In CR case, recrystallization took place through the thickness. Elongated grains are observed annealing at 280 °C in CR samples and when the cold-rolled sample started to recrystallize, a few newly recrystallized grains can be observed (Fig. 3a). After annealing at 320 °C, the cold-rolled sample is partly recrystallized (Fig. 3b). With increasing annealing temperature, recrystallization occurred quickly. After annealed at 360 °C, the deformed microstructure is fully recrystallized with slightly elongated grain structure (Fig. 3c). The annealing temperature also affects size and shape of recrystallized grains in cold-rolled 1050 aluminum alloy. At low temperatures, coarse, slightly elongated recrystallized grains are observed. With increasing annealing temperature, the size of the recrystallized grains decreases and recrystallized grains become gradually equiaxial.

As shown in Fig. 3 and 4, the microstructure evolution of both types of materials is similar under different annealing temperature. At the beginning of recrystallization, however, the development of microstructure through thickness is inhomogeneous in LTR-rolled materials. Recrystallized grains of LTR

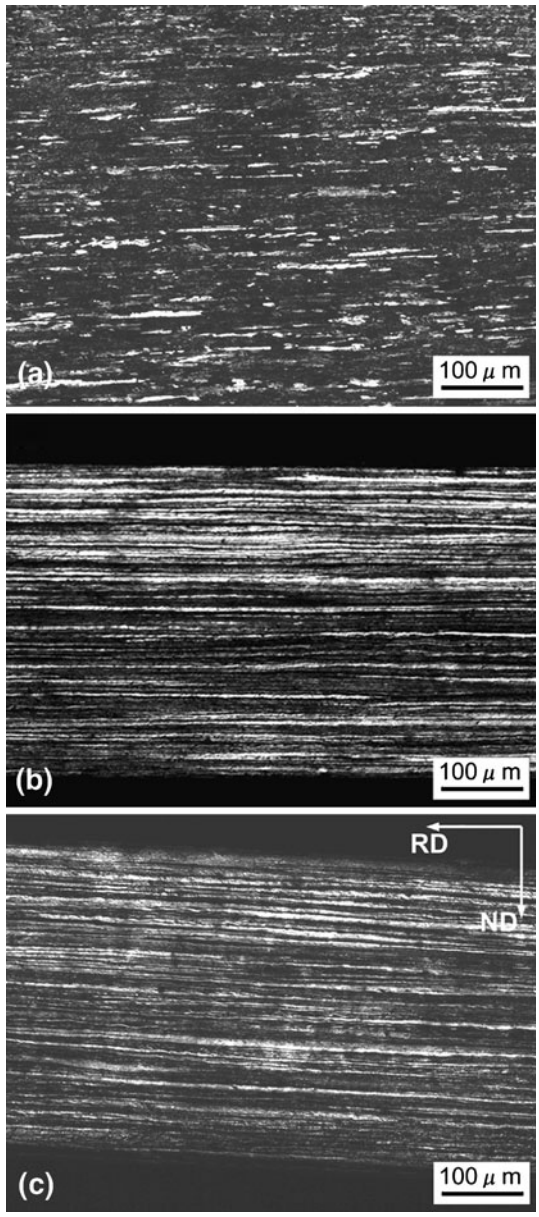

Fig. 1 Light microscopy images showing the microstructure of (a) CC hot band, (b) 93 pct reduction by CR, and (c) 93 pct reduction by LTR

samples are finer than those of CR samples. The part of deformed microstructure is recrystallized with some elongated grains in the intermediate and subsurface layers when annealing temperature is 280 °C (Fig. 4a). However, the deformed microstructure is not recrystallized in the center of the LTR sample.

The above phenomenon indicates that recrystallization takes place more easily in subsurface layer than in center. Compared to CR-rolled samples, the volume fraction of recrystallized grains is much larger, and the sizes of recrystallized grains are finer in LTR samples. With increasing annealing temperature, the volume fraction of recrystallized grains increases, and the inhomogeneity of microstructure through thickness decreases. After annealed at 360 °C, the deformed microstructure is fully recrystallized. But the inhomogeneity of microstructure through thickness is still observed. During recrystallization, the volume

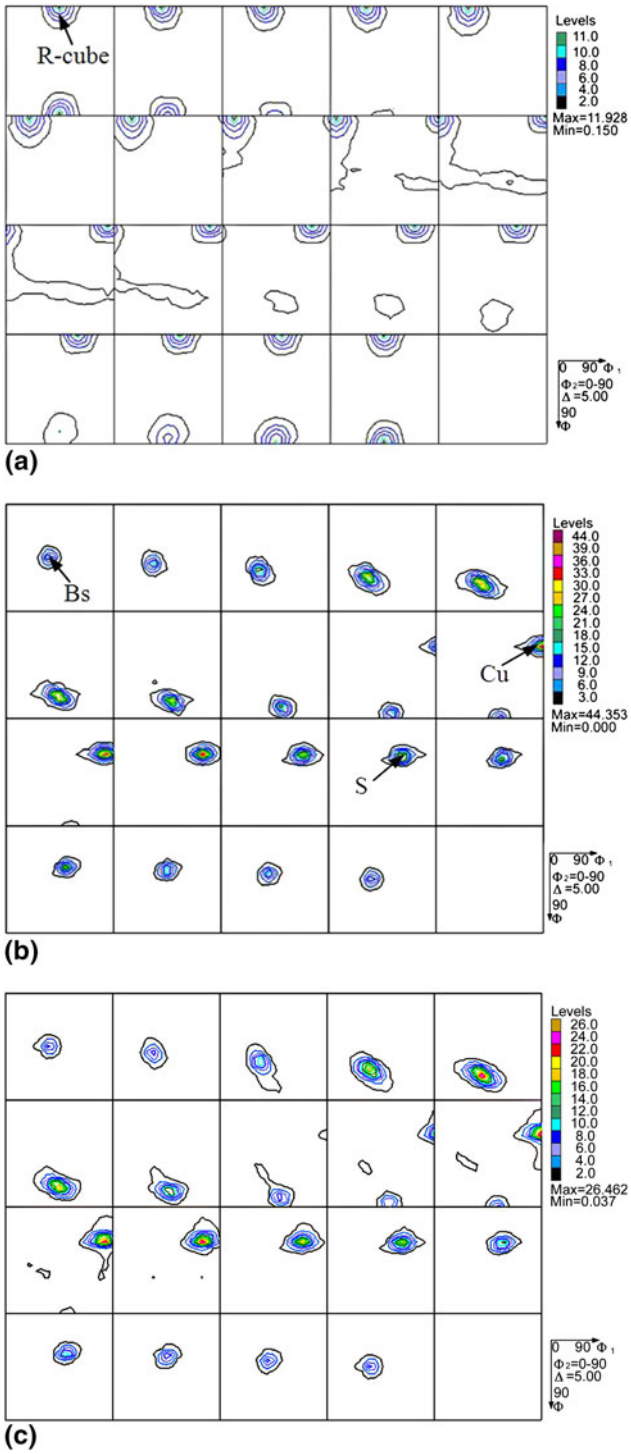

Fig. 2 ODFs of as-received 1050: (a) CC hot band, (b) 93 pct reduction by CR, and (c) 93 pct reduction by LTR

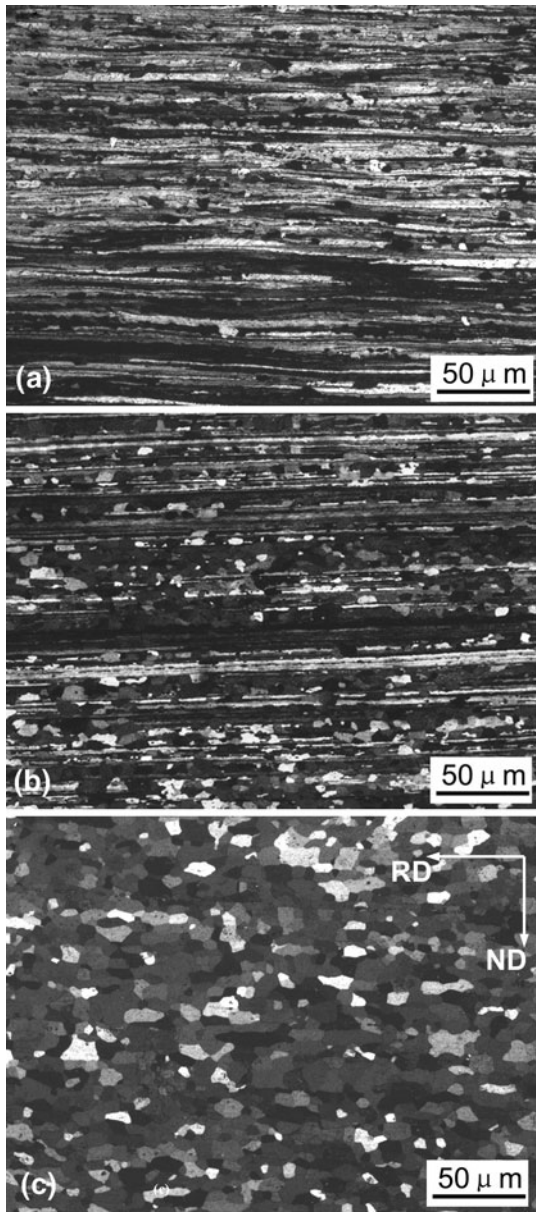

Fig. 3 Microstructure of CR-rolled 1050 aluminum alloy after annealing at (a) 280 °C, (b) 320 °C, and (c) 360 °C

fraction of recrystallized grains is higher in intermediate and subsurface layers than that in center, and the average recrystallized grain size is smaller in intermediate and subsurface layers.

3.2.2 Evolution of the Recrystallization Texture. Figure 5 shows the texture evolution of the CR- and LTR-rolled sample during annealing at different temperatures. Three sections of $\phi_2 = 0°$, $\phi_2 = 45°$, and $\phi_2 = 65°$ are selected to show the cube, R, copper, and S component. During annealing of the cold-rolled samples, recovery and recrystallization takes place. The β-fiber rolling texture is converted into a recrystallization texture. The texture is not changed during recovery period of the cold-rolled samples. The evolution of recrystallization texture is greatly influenced by the annealing temperature. For the CR-rolled samples, at low annealing temperature, the recrystallization texture mainly consists of β-fiber texture. The strength of β-fiber texture components decreases with increasing annealing temperature (such as the strength of Cu is 11 at 240 °C and decreased to 2 at 400 °C). After complete recrystallization at 400 °C, recrystallization texture has a strong cube component, weak R, and copper components.

For LTR-rolled samples, the texture evolution is different from that of CR-rolled samples. After annealed at 280 °C, the strength of β-fiber rolling texture decreases. The intensities of

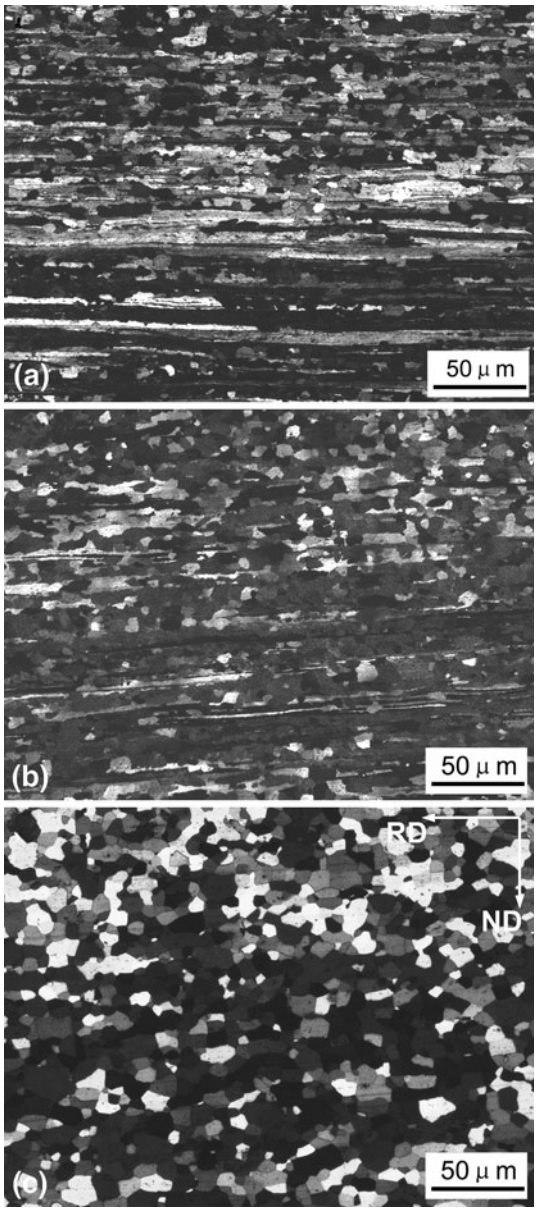

Fig. 4 Microstructure of LTR-rolled 1050 aluminum alloy after annealing at (a) 280 °C, (b) 320 °C, (c) 360 °C

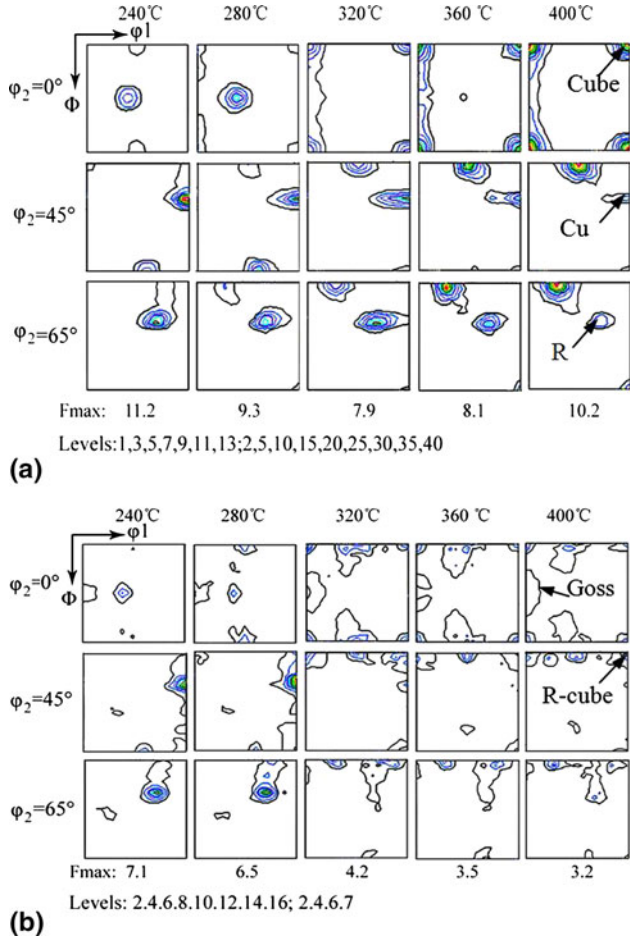

Fig. 5 Texture evolution of the cold-rolled 1050 aluminum alloy after annealing at different temperature: (a) CR-rolled samples and (b) LTR-rolled samples

orientation along β-fiber decrease, whereas the rotated cube appears with increasing annealing temperature. Moreover, the rotated cube component changes slightly with increasing annealing temperature. After complete recrystallization at 400 °C, the recrystallization textures of LTR sample has cube and rotated cube components, and the intensity of cube orientation is far lower than that of CR sample.

Figure 6(a) and (b) illustrates how the volume fractions of main texture components derived from the ODF changed after annealing at different temperature of those 1050 aluminum alloy rolled with CR and LTR. It is clear that the texture volume fractions are slightly varied with the annealing time during recovery. Texture volume fractions are changed greatly during recrystallization. For CR-rolled samples, the rolling texture is unchanged qualitatively in the early stages of annealing. It can be seen that during recovery state, the rolling texture components occupies much larger volume compared to the recrystallized texture components. During annealing treatment, the cube texture {001}⟨100⟩ evolves progressively with a simultaneous decrease of all main rolling texture components. After fully recrystallized, approximately 35.6% cube orientation is obtained. The change of microstructure after recrystallization with annealing temperature in LTR-rolled samples is not as significant as that in CR-rolled samples. During recrystallization, the volume fractions of β-fiber components decrease, whereas the cube components increase. But the volume fraction of Goss and R-cube components changed slightly after annealed at 320 °C. At fully recrystallized condition, the recrystallized textures contain approximately 7% cube and 5% rotated cube.

4. Discussion

It is well known that recrystallization takes place by the nucleation of dislocation free grains in the as-deformed microstructure and their subsequent growth into the neighboring deformed regions (Ref 13). Both nucleation and growth process of the recrystallized grains are thermally activated. This driving force is provided by the energy stored during the deformation. Recrystallization textures depend on the limited

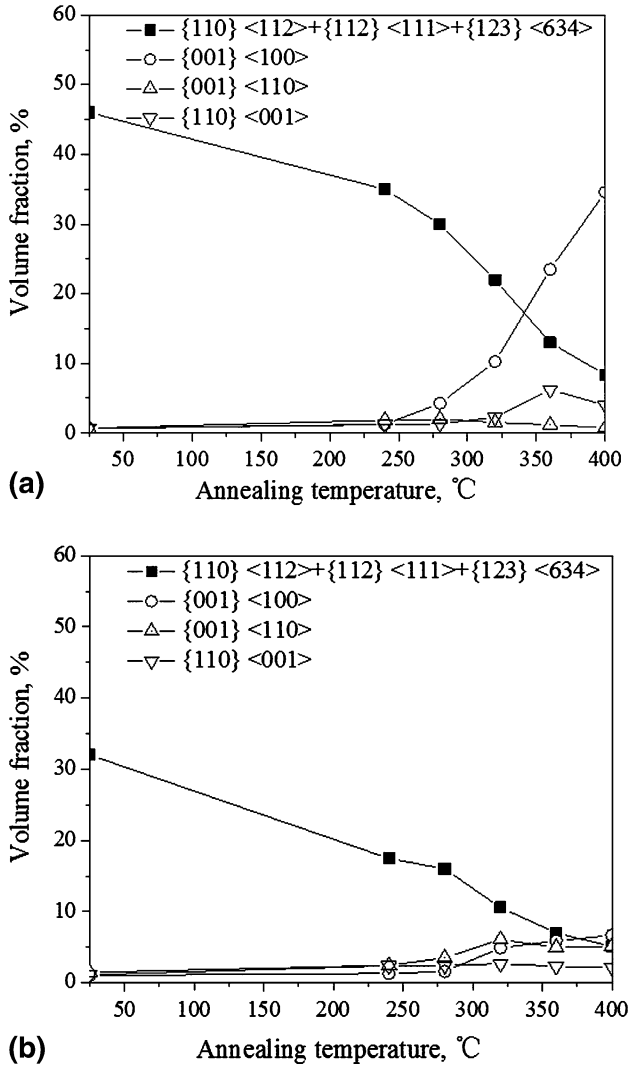

Fig. 6 The volume fractions of the texture components in the recrystallized specimens rolled with (a) CR and (b) LTR as a function of annealing temperature

spectrum of preferred nucleus orientations and the growth of nuclei that have the best growth conditions with respect to the surrounding matrix (Ref 14). The recrystallization textures of most Al alloys are dominated by the cube orientation, with strong scatter about the RD toward the Goss component. It is generally accepted that cube-oriented grains evolve from the cube bands present in the as-deformed microstructure (Ref 6, 9, 15). Another type of recrystallization texture found in aluminum alloys is the R texture, which exhibits almost the same position in Euler space as the former β-fiber rolling texture. The R-oriented grains are formed by nucleation within S-oriented grains at the grain boundaries between the deformation bands (Ref 14).

In the present experiments, CR and LTR specimens are rolled to the same final thickness. The deformation microstructures of two specimens are similar, but the microstructures and textures after recrystallization of two specimens show great difference. In CR sample, slightly coarse grained microstructure is obtained, and the microstructure through thickness is homogenous. In contrast, the recrystallization microstructure of LTR sample is finer, and the recrystallization texture along the sample thickness is more heterogeneous. This specimen shows that recrystallization texture mainly consists of only weaker cube orientation but stronger rotated cube and random orientation (Fig. 5b). As the rolling textures of both materials are virtually identical (Fig. 2), these strong microstructural and textural differences have obviously attributed to the imposed deformation on the surface of sheet in LTR sample.

During rolling with LTR, crater morphology of the textured roll surface is copied to the sheet and correspondingly form concave hole morphology on the surface of aluminum sheet. This imposed deformation increases dislocation density in the surface of sheet. Therefore, the cold-rolled sample of LTR should have a higher nucleation-site density and stored energy at the surface layer than that of CR samples. The higher stored energy in sheet surface would strongly accelerate recrystallization during annealing, which results in inhomogeneous microstructure in the thickness of LTR sheet. Furthermore, the high dislocation density in the surface of sheet might increase the activation energy for recrystallization, so the nucleation rate is enhanced during initial recrystallization stage. Furthermore, the high dislocation density in the surface of sheet will enhance recrystallization kinetics. So, the cube-oriented nucleus is decreased and the randomly oriented nucleus is increased. Accordingly, a weak cube orientation and a much higher fraction of random orientation are formed in the LTR sample.

5. Conclusions

The effect of laser texture on microstructure and texture of 1050 aluminum alloy during rolling and annealing is investigated. In the as-deformed state, textures of LTR- and CR-rolled materials are similar. Upon annealing, recrystallization texture was strongly changed in LTR sample, and recrystallization produced a finer grain size and weaker recrystallization texture than that in the CR sample. The major findings are summarized as follows:

(i) The recrystallization microstructure of 1050 aluminum alloy rolled with LTR shows slightly finer and more inhomogeneous grains through the thickness than that of 1050 aluminum alloy rolled with CR.

(ii) The recrystallization textures of 1050 aluminum alloy rolled with CR are characterized by the R orientation and strong cube orientation with scattering about RD toward the Goss orientation. In comparison, the recrystallization textures of 1050 aluminum alloy rolled with LTR exhibit weaker cube and Goss components and stronger rotated cube component as well as a much higher fraction of randomly oriented grains.

(iii) The changes in texture through recrystallization are mainly shown by the difference of rolling and recrystallization texture components. For the 1050 aluminum alloy rolled with CR, recrystallization decreases and the strength of the β-fiber component and the rotated cube component, but increases the cube, R, and Goss components. For the 1050 aluminum alloy rolled with LTR, recrystallization increases volume fraction of cube and rotated cube texture components at the expense of β-fiber component, but the Goss component changes slightly during recrystallization.

Acknowledgments

The authors are grateful to acknowledge the financial support of the Key Technologies R&D Program of Harbin (No. 2006AA4CG021) and the Innovative fund for youth of Harbin (No. 2006RFQGG060).

References

1. M.J. Yang, Developing Technology of YAG Laser Textured Roll and Its Application, *Proceedings of the 2nd APEC SME Technology Conference* (Yantai, China), 1998, p 27–31
2. Z.Y. Li, M.J. Yang, W.J. Liu, and M.L. Zhong, Investigation on Crater Morphology by High Repetitive Rate YAG Laser-Induced Discharge Texturing, *Surf. Coat. Technol.*, 2006, **200**, p 4493–4499
3. Z.G. Lin, The Experimental Study of Laser Microprecision Treatment of I.C. Engine Tappet, *Tribol. Trans.*, 1994, **37**(2), p 430–432
4. M. Geiger, S. Roth, and W. Becker, Influence of Laser-Produced Microstructure on the Tribology Behavior of Ceramics, *Surf. Coat. Technol.*, 1998, **100**, p 17–22
5. N. Hansen and D.J. Jensen, Deformation and Recrystallization Textures in Commercially Pure Aluminum, *Metall. Trans. A*, 1986, **17**(2), p 253–259
6. H.E. Vatne, R. Shahanf, and E. Nes, Deformation of Cube-Oriented Grains and Formation of Recrystallized Cube Grains in a Hot Deformed Commercial AlMgMn Aluminium Alloy, *Acta Mater.*, 1996, **44**(11), p 4447–4462
7. J. Hirsch and K. Lucke, The Application of Quantitative Texture Analysis for Investigating Continuous and Discontinuous Recrystallization Processes of Al0.01Fe, *Acta Metall.*, 1985, **33**(10), p 1927–1938
8. K. Lucke, Formation of Recrystallization Textures in Metals and Alloys, *Proceedings of 7th International Conference on Textures of Materials (ICOTOM 7)*, Netherlands Society of Materials Science, Zwijndrecht, 1984, p 195–210
9. K. Lucke, Orientation Dependence of Grain Boundary Motion and the Formation of Recrystallization Textures, *Can. Metall. Q.*, 1974, **13**, p 261–274
10. O. Daaland and E. Nes, Recrystallization Texture Development in Commercial Al-Mn-Mg Alloys, *Acta Mater.*, 1996, **44**(4), p 1413–1435
11. Z.D. Liang, J.Z. Xu, and F. Wang, Determination of ODF of Polycrystalline Materials from Incomplete Pole Figures, *Proceedings of the 6th International Conference on Textures of Materials (ICOTOM 6)*, Iron and Steel Institute of Japan, Tokyo, 1981, p 1259–1265
12. D.J. Jensen, N. Hansen, and F.J. Humphrey, Texture Development During Recrystallization of Aluminium Containing Large Particle, *Acta Metall.*, 1985, **33**(11), p 2155–2162
13. H.E. Vatne and E. Nes, The Origin of Recrystallization Texture and the Concept of Micro-growth Selection, *Scripta Metall. Mater.*, 1994, **30**(3), p 309–312
14. E. Nes and J.K. Solberg, Growth of Cube Grain During Recrystallization in Aluminium, *Mater. Sci. Technol.*, 1996, **2**(1), p 19–21
15. B.J. Duggan, K. Lücke, K. Lücke, G. Koehlhoff, and C.S. Lee, On the Origin of Cube Texture in Copper, *Acta Metall. Mater.*, 1993, **41**(6), p 1921–1927